Vegetable Research

ARTICLE

Open Access

https://doi.org/10.48130/vegres-0026-0006

Vegetable Research **2026**, 6: e017

Transcriptomic analysis reveals lignin-associated genes involved in ToBRFV-induced brown hardened spots and defense in tomato fruit

Xueying Cao[1,2], Jun Ren[2*], Kun Yang[2], Yun Yu[2], Tingting Zheng[2], Zizheng Wang[2], Shenzao Fu[2], Aiai Li[2] and Zhe Wu[1*]

[1] *College of Horticulture, Shanxi Agricultural University, Taigu 030801, China*

[2] *State Key Laboratory of Vegetable Biobreeding, Institute of Vegetables and Flowers, Chinese Academy of Agricultural Sciences, Beijing 100081, China*

* Correspondence: renjun@caas.cn (Ren J); wzz0618@163.com (Wu Z)

Abstract

Tomato brown rugose fruit virus (ToBRFV) represents a significant threat to global tomato production, resulting in decreased yields and compromised fruit quality due to the formation of brown, hardened spots on infected fruit. This study aimed to elucidate the molecular mechanisms for ToBRFV-induced lesions in tomato fruit using transcriptome sequencing and virus-induced gene silencing (VIGS) techniques. Transcriptome analysis was conducted on tomato fruit at green-ripe (L), and red-ripe (H) stages, examining three tissue types: brown lesions (B), non-brown areas of infected fruit (BC), and healthy controls (CK). A total of 34 differentially expressed genes (DEGs) related to phenylpropanoid biosynthesis were identified, with *PAL* (*Solyc05g056170.3*), *C4H* (*Solyc05g047530.3*), *CAD* (*Solyc02g069250.3*), and *POD* (*Solyc02g094180.3*) showing the highest transcript abundances in brown lesion tissues.

Crucially, silencing *POD* (*Solyc02g094180.3*) increased tomato susceptibility to ToBRFV, accompanied by increased accumulation of hydrogen peroxide (H_2O_2), and superoxide anions ($O_2^{\bullet-}$). In contrast, silencing *PAL* (*Solyc05g056170.3*), *C4H* (*Solyc05g047530.3*), *or CAD* (*Solyc02g069250.3*) improved resistance and suppressed viral accumulation. Collectively, these findings indicate that these four genes are crucial regulators of lignin biosynthesis in tomato, and that the brown hardened lesions induced by ToBRFV are associated with lignin accumulation. Furthermore, POD plays a vital role in mediating resistance to ToBRFV by regulating reactive oxygen species. This study provides important insights into the molecular responses of tomato fruit, laying a foundation for breeding ToBRFV-resistant tomato varieties with improved fruit quality.

Citation: Cao X, Ren J, Yang K, Yu Y, Zheng T, et al. 2026. Transcriptomic analysis reveals lignin-associated genes involved in ToBRFV-induced brown hardened spots and defense in tomato fruit. *Vegetable Research* 6: e017 https://doi.org/10.48130/vegres-0026-0006

Introduction

Tomato (*Solanum lycopersicum* L.) is one of the most economically important vegetable crops globally, significantly contributing to dietary health and nutrition[1–3]. According to statistics from the Food and Agriculture Organization (FAO), global tomato production reached 47 million metric tons in 2024, resulting in a market size of approximately 50 billion USD, with projections indicating it may exceed 70 billion USD by 2028, growing at a compound annual growth rate (CAGR) of 6%. As a major tomato-producing country, China accounts for over one-third of global output (66 million tons), and holds 12% of the global trade value in processed tomato products. This underscores the vital role the tomato industry plays in the national agricultural economy and global food security. However, tomato production faces numerous challenges, particularly from various biotic stresses, with viral diseases being among the most detrimental factors, resulting in significant yield reductions and a decline in fruit quality[4,5]. The tomato brown rugose fruit virus (ToBRFV), a recently identified member of the *Tobamovirus* genus, was first detected in Israel in 2014 and has since rapidly disseminated across numerous countries and regions, posing a transboundary agricultural threat[6–8]. Infection typically manifests through a range of symptoms, most notably manifesting in both leaves and fruit, leading to diminished crop vigor, compromised fruit quality, and substantial economic losses. Infected tomato fruit frequently exhibit abnormal pigmentation, characterized by brown, hardened spots, which detract from marketability and reduce nutritional value[5–9]. Due to its high transmissibility, broad host range, and ability to overcome the conventional *Tm-2* resistance gene in tomatoes, ToBRFV has been designated as a regulated quarantine pest in many regions and is currently viewed as one of the most significant threats to the global tomato industry[5,6,8,9]. Despite substantial research efforts focused on transmission pathways, host range, and strategies for resistance development, the underlying molecular mechanisms responsible for the formation of brown lesions associated with ToBRFV infection remain poorly understood. Investigations into the genetic and biochemical pathways implicated in symptom expression are notably limited[4–10].

Recent advancements in high-throughput transcriptome sequencing (RNA-seq) have opened new avenues for exploring gene expression dynamics within infected plants[11–13]. Transcriptomic analyses can provide insights into the intricate regulatory networks that govern plant defenses during viral infections[14–18]. Previous research has underscored the importance of the phenylpropanoid biosynthesis pathway in mediating plant immune responses, with key enzymes such as phenylalanine ammonia-lyase (PAL), cinnamate 4-hydroxylase (C4H), and peroxidase (POD) playing crucial roles[19,20]. This pathway is responsible for producing a variety of metabolites, including lignin, flavonoids, and phenolic acids, among which lignin serves as a major component of the plant cell wall and acts as a physical barrier against pathogen invasion[21–23]. Key enzymes in the phenylpropanoid biosynthesis pathway, including PAL, C4H, 4-coumaroyl CoA ligase (4CL), cinnamyl-alcohol dehydrogenase (CAD), and POD have been closely linked to lignin accumulation and plant disease resistance[20,24,25]. For instance, silencing *PAL* or *CAD* genes in plants results in reduced lignin content and heightened

susceptibility to pathogens[12,26], while overexpression of *POD* promotes lignin deposition and enhances disease resistance[27]. However, the role of the phenylpropanoid biosynthesis pathway and its key enzymes in the development of brown hardened lesions and resistance to ToBRFV in tomato fruit remains to be elucidated.

In this study, we aimed to investigate the molecular responses of tomato fruit to ToBRFV infection by performing a comprehensive transcriptomic analysis on different tissues (brown lesions, non-brown areas of infected fruits, and healthy controls) at distinct ripening stages. We specifically focused on genes associated with the phenylpropanoid biosynthesis pathway, linking changes in expression to lignin content and susceptibility to ToBRFV infection. Our findings highlight key genes involved in the formation of brown necrotic spots and contribute to a broader understanding of the response mechanisms of tomato fruit to viral pathogens. Ultimately, this research may provide essential insights for developing breeding strategies aimed at producing resistant cultivars against ToBRFV-induced damage.

Materials and methods

Plant material

The experimental tomato plants used in this study were cultivated in a controlled-environment growth chamber at the Institute of Vegetables and Flowers, Chinese Academy of Agricultural Sciences (IVF-CAAS), Beijing, China. Throughout the growth period, the diurnal temperature was regulated between 22 and 30 °C during the day and 18 to 25 °C at night, natural light was utilized, and the relative humidity was maintained at 60% ± 10%. Tomato plants were inoculated with ToBRFV provided by the Plant Variety Testing Group at IVF-CAAS. All inoculation experiments were conducted in a sealed plant growth chamber under stringent quarantine conditions to avoid cross-contamination. The experimental design included two treatment groups: the inoculated group, where tomato leaves were mechanically inoculated with ToBRFV using carborundum-assisted rubbing, and a control group, which consisted of leaves mock-inoculated with sterile water following the same technique. Samples were collected from healthy green fruit (LCK), infected fruit displaying no visible symptoms (LBC), and infected fruit showing abnormal coloration (LB). At the red fruit stage, corresponding samples were taken from healthy red fruit (HCK), infected fruit with normal pigmentation (HBC), and infected fruit exhibiting discolored, necrotic areas (HB) (Fig. 1). All samples were promptly separated and immediately frozen in liquid nitrogen. Three biological replicates were prepared for each collection time point.

RNA-seq analysis

RNA extraction for transcriptome sequencing was performed using TRIzol reagent (Thermo Fisher, Cat. No. 1559601) according to the manufacturer's recommended protocol. The cDNA library for sequencing was accomplished utilizing a pair-ended sequencing approach, carried out by LC Sciences (Hangzhou, China)[28]. To ensure the quality of sequencing data, low-quality reads were filtered using Cutadapt (version 1.9)[29], and FastQC (version 0.11.9)[30] to ensure data integrity. The transcriptome sequences were aligned and statistically analyzed against the tomato reference genome using HISAT2[31] and StringTie[32]. Principal Component Analysis (PCA) was performed to assess sample correlations, utilizing the FactoMineR package in R. The fragments per kilobase of transcript per million mapped reads (FPKM) method was employed to quantify gene expression levels. Differential expression analysis was conducted with DESeq2 software[33,34], employing thresholds of $|\log_2\text{FoldChange}| > 1$, and p-value ≤ 0.05. The transcripts were annotated utilizing various databases, including NCBI NR, Swiss-Prot, KEGG, GO, Pfam, and KOG. Following this, the DEGs were analyzed for enrichment in Gene Ontology (GO) functions and Kyoto Encyclopedia of Genes and Genomes (KEGG) pathways. All RNA sequencing experiments were performed with three biological replicates for each experimental condition.

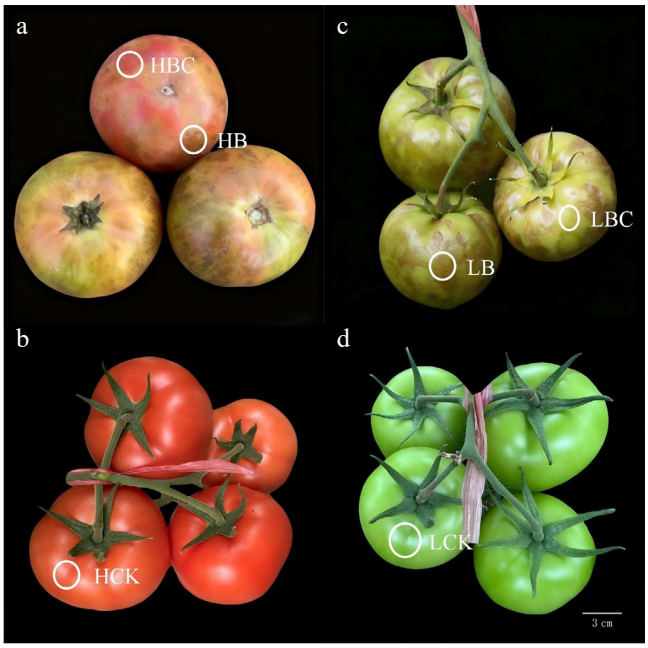

Fig. 1 Schematic diagram of sample collection for transcriptome sequencing. Fruit tissues were selected at two key growth stages: green-ripe (L) and red-ripe (H), and divided into six sample groups: green-ripe diseased brown areas (LB), green-ripe diseased non-brown areas (LBC), green-ripe healthy controls (LCK), red-ripe diseased brown areas (HB), red-ripe diseased non-brown areas (HBC), and red-ripe healthy controls (HCK).

Quantitative real-time PCR (qRT-PCR) analysis

Total RNA was extracted using the Simple Total RNA Extraction Kit (Tiangen, Beijing, China) in accordance with the manufacturer's instructions. The concentration and purity of the RNA were evaluated with a NanoDrop 2000 Spectrophotometer (Molecular Devices, Santa Clara, CA, USA). Complementary DNA (cDNA) was synthesized by reverse transcription using the PrimeScript™ RT reagent kit (Perfect Real Time) (TaKaRa, Dalian, China). Primer Premier 5.0 was employed for the design of qRT-PCR primers, which were subsequently synthesized by Sangon Biotech Co., Ltd. (Shanghai, China). Detailed primer information is provided in Supplementary Table S1. Only primers with amplification efficiencies between 90% and 110% were used, with Actin as the internal reference gene (Supplementary Table S1). qRT-PCR reactions were run on an Applied Biosystems 7500 thermocycler (Thermo Fisher Scientific, Waltham, MA, USA) with TIANGEN Biotech's SYBR Green PCR Master Mix (Beijing, China). Data analysis was conducted using QuantStudio Design & Analysis Software to obtain raw quantification cycle (Cq) values. Relative expression levels were calculated using the $2^{-\Delta\Delta CT}$ method[35], with each sample analyzed in three biological replicates and four technical replicates.

Virus-induced gene silencing (VIGS) in tomato

For VIGS, we utilized the SGN VIGS Tool (https://vigs.solgenomics.net) to design optimal target-specific sequences[20]. A 300 bp target fragment was digested using EcoRI and BamHI, and subsequently ligated into the tobacco rattle virus RNA2 (TRV2) vector. The recombinant vectors were transformed into *Agrobacterium tumefaciens* strain GV3101, and the subsequent culture conditions were set according to the established protocols described by Jiang et al.[36] and Wang et al.[12]. For VIGS assays, a mixed suspension of *A. tumefaciens* containing TRV1 and TRV2 carrying the respective fragments, was syringe-infiltrated into the leaf tissues of MM tomato seedlings at the 4–6 leaf growth stage. The tomato *phytoene desaturase* (*PDS*) gene was selected as a positive control to confirm the efficiency of gene silencing[37], while *A. tumefaciens* carrying an empty TRV1 vector acted as a negative control.

After infiltration, leaf samples from the treated plants were collected 14 d post-infiltration (dpi) for RNA extraction. qRT-PCR was performed to evaluate the efficacy of gene silencing. The VIGS-treated plants were then inoculated with ToBRFV 14 dpi, and leaf phenotypes were assessed at 20 dpi. Three independent biological replicates were conducted, with more than 15 plants analyzed in each treatment. All primers used for VIGS are listed in Supplementary Table S1.

Extraction and determination of lignin

Fresh tomato leaves from each experimental group were collected, and dried in an oven at 80 °C for 48 h until fully desiccated. The dried leaves were then ground into a fine powder and passed through a 40-mesh sieve. Approximately 5 mg of the powdered sample was weighed and transferred into a 1.5 mL centrifuge tube. Lignin content was assessed using the Lignin Content Detection Kit (Solarbio#BC4200, Solarbio Science & Technology Co., Ltd., Beijing, China), following the manufacturer's protocol. Briefly, the sample was treated with acetyl bromide in acetic acid solution at 80 °C for 40 min. Following centrifugation at 8,000 g for 10 min, the supernatant was collected and diluted with glacial acetic acid to create the test solution. Prior to spectrophotometric measurement, the spectrophotometer was preheated for at least 30 min, set to 280 nm, and zero-adjusted using glacial acetic acid. The lignin content was quantified for further data analysis.

ROS content detection

Histochemical detection of reactive oxygen species (ROS) accumulation in tomato tissues was conducted following standard staining protocols, with three biological replicates for all assays. Hydrogen peroxide (H_2O_2) was localized using Diaminobenzidine (DAB) staining. Leaf samples from ToBRFV -infected tomato plants (treatment group) and healthy, uninfected leaves (control group) were excised and immersed in freshly prepared 1 mg/mL DAB working solution, made by dissolving 100 mg of DAB powder in 100 mL of deionized water (ddH_2O), and kept in the dark. To ensure uniform penetration, samples underwent vacuum infiltration for 2 h. After incubation in the dark, samples were decolorized by boiling in anhydrous ethanol, with the ethanol replaced every five min until all chlorophyll was completely removed, resulting in white tissue that clearly displayed the DAB polymer precipitate[38]. The accumulation of superoxide anion radical ($O_2^{\bullet-}$) was visualized using Nitroblue Tetrazolium (NBT) staining. An NBT stock solution (0.5 mg/mL) was prepared by dissolving 50 mg of NBT in 100 mL of ddH_2O, and samples were immersed and subjected to vacuum infiltration for 8 h. Following staining, the samples were decolorized using the same ethanol boiling method described previously[39]. Final stained samples were mounted and documented using a flatbed scanner. The methods for detecting H_2O_2 and $O_2^{\bullet-}$ content were carried out according to the instructions of the H_2O_2 Content Detection Kit and the $O_2^{\bullet-}$ Content Detection Kit, respectively, from Beijing Solarbio Technology Co., Ltd.

Results

Evaluation of transcriptome data

Transcriptome sequencing was performed on tomato fruit RNA at different fruit tissues (HB, HBC, HCK, LB, LBC, and LCK). The value of Q20 for each group was no less than 99.98%, and the value of Q30 was generally above 97.95%. These values were positively correlated with the sequencing quality. The percentages of GC content were 42%, 41.50%, 41.50%, 41.50%, 43%, and 42%, respectively (Supplementary Table S2).

To assess sample correlation and biological repeatability, Pearson's correlation coefficient was calculated and visualized in Fig. 2. As illustrated, the data points for LCK, LBC, and LB were dispersed across different quadrants, while the points for HCK, HBC, and HB clustered distinctly within the same quadrant. High inter-replicate correlations were observed in each group, confirming the robustness of the biological replicates utilized in this study.

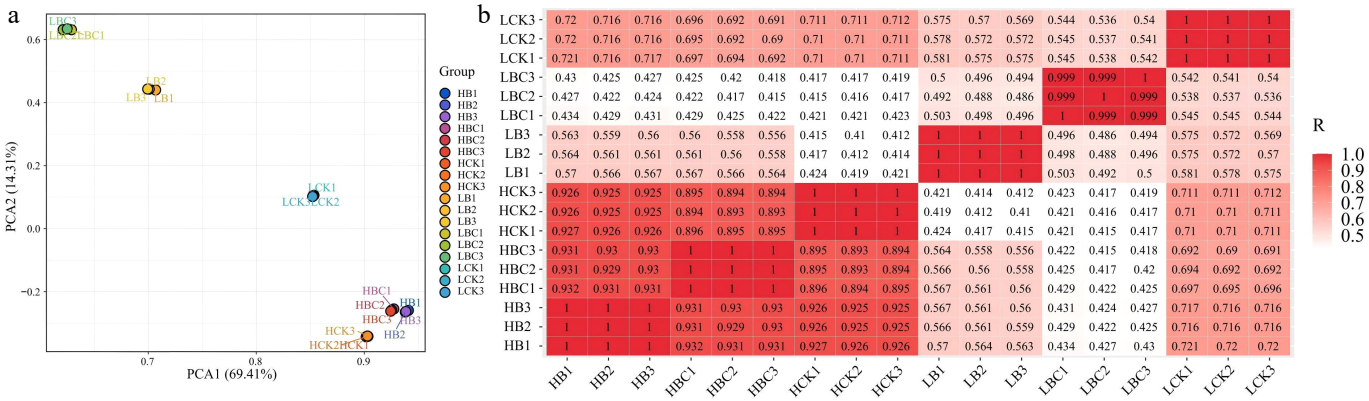

Fig. 2 Correlations among sample replicates from different tissues. (a) Two-dimensional principal component analysis (PCA) plot. (b) Heatmap illustrating Pearson correlation coefficients.

DEGs between different tissues

The DEGs were identified using DESeq2 software across six different groups, as well as edgeR for comparisons between two samples. Genes with a false discovery rate (FDR) of less than 0.05 and an absolute fold change of ≥ 2 were classified as differentially expressed.

During the red fruit stage of tomato fruit, in the HB vs. HCK comparison, a total of 3,636 DEGs were identified (1,821 upregulated and 1,815 downregulated); in the HBC vs. HCK comparison, a total of 3,895 DEGs were identified (2,002 upregulated, 1,893 downregulated) (Fig. 3a–c). In the green fruit stage of tomato fruit, the number of DEGs between LB and LCK was 5,345, the number of DEGs between LBC and LCK was 4,926, and the number of DEGs between LB and LBC was 2,427 (Fig. 3d–f). Furthermore, in the green fruit stage of tomato, there were 557 common DEGs among the three sample groups, while in the red fruit stage, 441 DEGs were commonly shared across the three sample groups (Fig. 3c, f).

GO annotation and KEGG enrichment analysis of DEGs

To investigate the biological significance of DEGs, GO enrichment analysis was implemented on DEGs. In all group comparisons, the DEGs were predominantly enriched in biological process (BP) and molecular function (MF) categories. For instance, the top 20 DEGs identified in the HB vs. HCK comparison included annotations for nine BP-related terms, four cellular component (CC)-related terms, and seven MF-related terms (Fig. 4a). In the HB vs. HBC comparison, the top 20 DEGs were associated with six BP-related terms, three CC-related terms, and 11 MF-related terms (Fig. 4b). Similarly, the top 20 DEGs from the HBC vs. HCK comparison contained seven BP-related terms, four CC-related terms, and nine MF-related terms (Fig. 4c). For the LB vs. LCK comparison, these genes included seven BP-related terms, five CC-related terms, and eight MF-related terms (Fig. 4d). The LB vs. LBC comparison revealed seven BP-related terms, four CC-related terms, and nine MF-related terms among the top 20 DEGs (Fig. 4e), while the LBC vs. LCK comparison identified nine BP-related terms, three CC-related terms, and eight MF-related terms (Fig. 4f). Notably, ten functional groups were consistently observed across multiple comparisons, including: oxidoreductase activity, heme binding, chitin binding, hydrolase activity, hydrolyzing O-glycosyl compounds, hydrolase activity acting on glycosyl bonds, metabolic processes, lipid metabolism, xyloglucan metabolic process, carbohydrate metabolic process, and integral component of membranes (Fig. 4).

KEGG serves as a comprehensive database that integrates genomic, chemical, and functional information, allowing for the analysis of the expression of differentially expressed genes (DEGs) involved in various biological pathways. The top 20 pathways with the most significant enrichment are presented in Fig. 5. Across all group comparisons, the DEGs were primarily enriched in pathways related to plant hormone signal transduction, metabolic processes, biosynthesis of secondary metabolites, phenylpropanoid biosynthesis, and flavonoid biosynthesis.

Gene expression patterns of phenylpropanoid and flavonoid biosynthesis pathways in different tomato fruit tissues

In the GO annotation and KEGG enrichment analysis of different tissues of ToBRFV-infected fruits, the secondary metabolic process (phenylpropanoid and flavonoid biosynthesis pathways) was mainly involved. In this study, 34 DEGs related to phenylpropanoid metabolism in different tissues of ToBRFV-infected fruits were identified, including *phenylalanine ammonialyase* (*PAL*), *cinnamate 4-hydroxylase* (*C4H*), *4-coumaroyl CoA ligase* (*4CL*), *cinnamoyl-CoA reductase* (*CCR*), *cinnamyl-alcohol dehydrogenase* (*CAD*), *peroxidase* (*POD*), *shikimate O-hydroxycinnamoyltransferase* (*HCT*), *5-O-(4-coumaroyl)-d-quinate3-monooxygenase* (*C3'H*), *caffeicacid3-O-methyltransferase* (*COMT*), and *caffeoyl-CoAO-methyltransferase* (*CCOAOMT*). Based on the reported biosynthesis pathways of phenylpropanoids and flavonoids in model plants, we constructed a regulatory network diagram of DEGs (Fig. 6).

A comparative analysis demonstrated that *PAL* (*Solyc05g056170.3*), *C4H* (*Solyc05g047530.3*), *4CL* (*Solyc03g111170.3*, *Solyc03g097030.3*), *POD* (*Solyc05g052280.3*, *Solyc06g050440.3*), and *C3'H* (*Solyc10g078220.2*, *Solyc01g096670.3*) exhibited significantly higher expression levels in the infected group (B, BC) compared to the control group (CK). *CAD* (*Solyc02g069250.3*) and *POD* (*Solyc02g094180.3*) exhibited significantly higher expression levels in the infected group (B), compared to the other two groups (BC and CK). *4CL* (*Solyc11g069050.2*), *POD* (*Solyc02g080530.3*, *Solyc08g069040.3* and *Solyc07g047740.3*), and *CCoAOMT* (*Solyc10g050160.2*) showed downregulated expression after infection at both the green fruit stage and the red fruit stage. *PAL* (*Solyc10g086180.2*), *POD* (*Solyc11g010120.2*), and *COMT* (*Solyc01g080180.3*) showed higher expression after infection at the red fruit stage and downregulated expression after infection at the green fruit stage. *POD* (*Solyc03g006810.3* and *Solyc09g007520.3*) showed higher expression after infection at the green fruit stage and downregulated expression after infection at the red fruit stage (Fig. 6).

Identification of candidate genes

We validated the reliability of the RNA-seq results, using qRT-PCR to examine the expression levels of four genes (*Solyc10g086180.2*, *Solyc01g096670.3*, *Solyc03g097030.3*, and *Solyc01g006300.3*) involved in the phenylpropanoid biosynthesis pathway. The expression patterns in different tomato fruit tissues obtained by RT-qPCR were similar to those obtained by RNAseq, which suggested that transcriptome data was reliable and valid (Fig. 7). Moreover, *PAL* (*Solyc05g056170.3*) and *C4H* (*Solyc05g047530.3)* exhibited significantly higher expression levels in the infected group (B, BC) compared to the control group (CK). In addition, *CAD* (*Solyc02g069250.3*) and *POD* (*Solyc02g094180.3*) showed significantly elevated expression levels in the infected group (B) relative to both BC and CK groups. These findings suggest that these four genes may play crucial roles in tomato defense against ToBRFV infection.

Effects of silencing candidate genes on the phenylpropanoid biosynthesis pathway and resistance in response to ToBRFV

Four candidate genes were temporarily silenced by VIGS, to explore their roles in lignin biosynthesis and resistance to ToBRFV. Twenty one days following vacuum infestation with *pTRV2-PDS*, the plants displayed clear signs of chlorosis and whitening symptoms, demonstrating the effectiveness of virus inoculation in silencing the plants (Fig. 8a). Additionally, the transcription of these four genes was significantly downregulated in silenced plants compared with the control (CK, negative plant), with silencing efficiencies ranging from −41% to −79%, indicating that the *pTRV-VIGS* system was successfully established (Fig. 8b). Subsequent analysis demonstrated a notable reduction in lignin content in the plants after silencing these genes (Fig. 8c).

To further investigate the roles of these genes in tomato response to viral infection, ToBRFV was mechanically inoculated onto the 3rd and 4th upper leaves of plants in each treatment group. Symptom

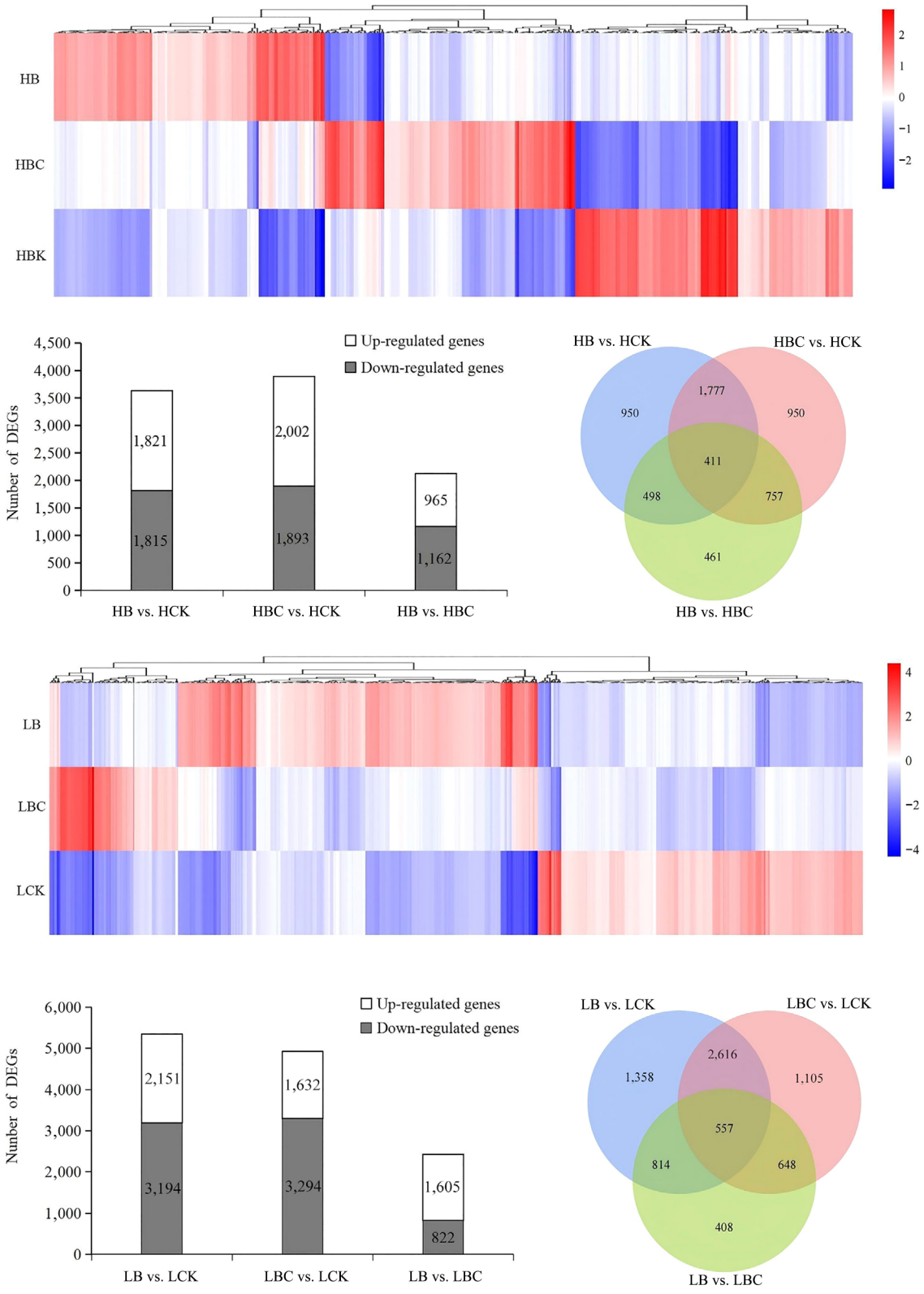

Fig. 3 Transcriptional response statistics of tomato tissues. (a) Differentially expressed gene heatmap on red-ripe (H). (b) Differentially expressed gene number on red-ripe (H). (c) Venn analysis of differentially expressed genes among the different tissues on red-ripe (H). (d) Differentially expressed gene heatmap on green-ripe (L). (e) Differentially expressed gene number on green-ripe (L). (f) Venn analysis of differentially expressed genes among the different tissues on green-ripe (L).

observation revealed that at 7 dpi, all groups exhibited mild downward leaf curling; by 14 dpi, symptoms had progressed to leaf narrowing and pronounced crinkling (Fig. 8d). Notably, compared with the *TRV2-GFP* control group, the *TRV-POD*-silenced plants displayed more severe leaf curling, whereas plants silenced for *CAD*, *C4H*, or *PAL* showed milder symptoms.

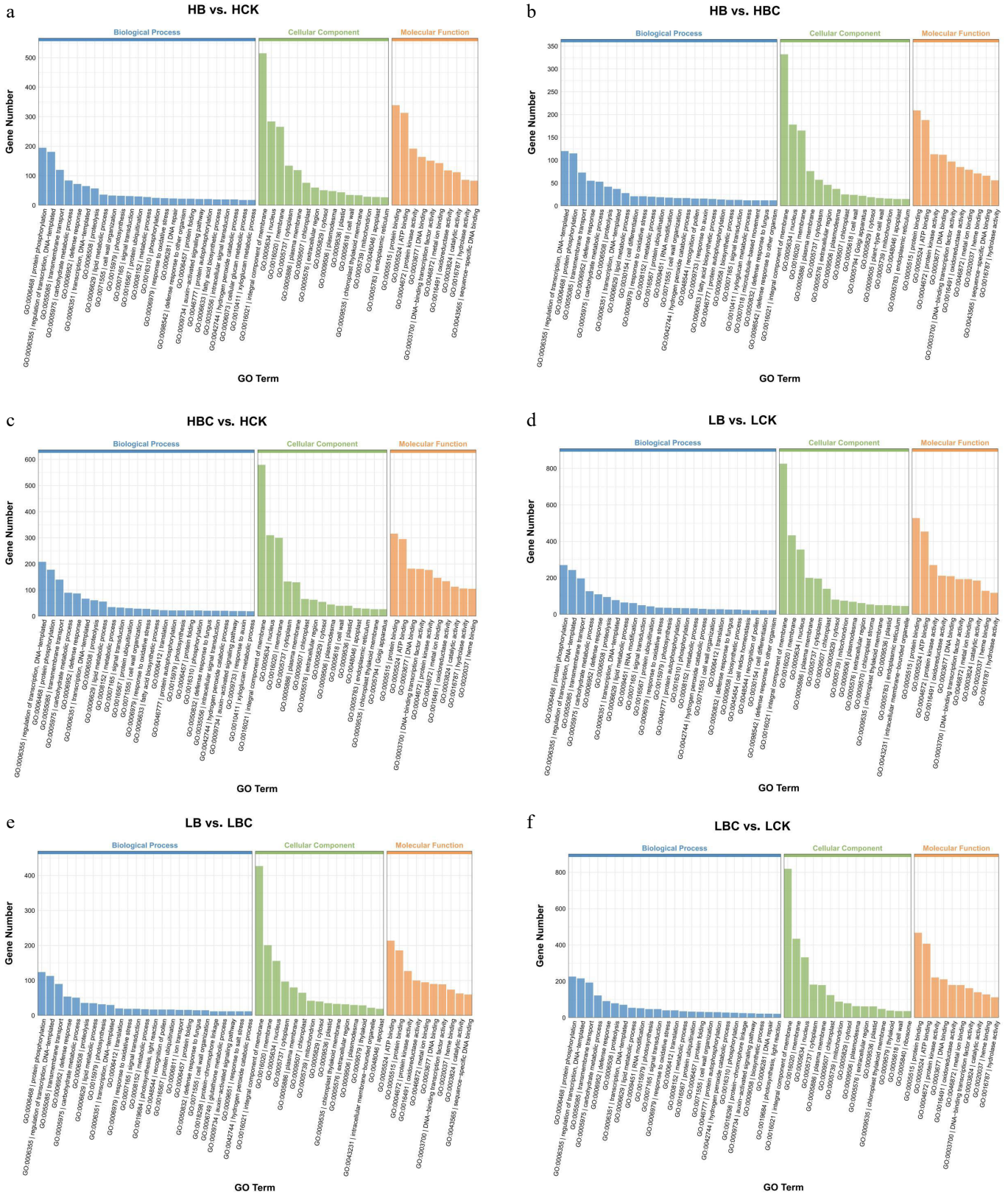

Fig. 4 GO annotation of DEGs between sample replicates within each tissue of tomato fruit. (a) HB vs. HCK, (b) HB vs. HBC, (c) HBC vs. HCK, (d) LB vs. LCK, (e) LB vs. LBC, (f) LBC vs. LCK.

To validate viral infection efficiency, quantitative primers were designed to measure viral accumulation. As shown in Fig. 8e, viral load was significantly higher in the *TRV-POD* group than in the *TRV2-GFP* control, while it was significantly lower in the *TRV-CAD*, *TRV-C4H*, and *TRV-PAL* groups. These results were consistent with the observed phenotypic differences.

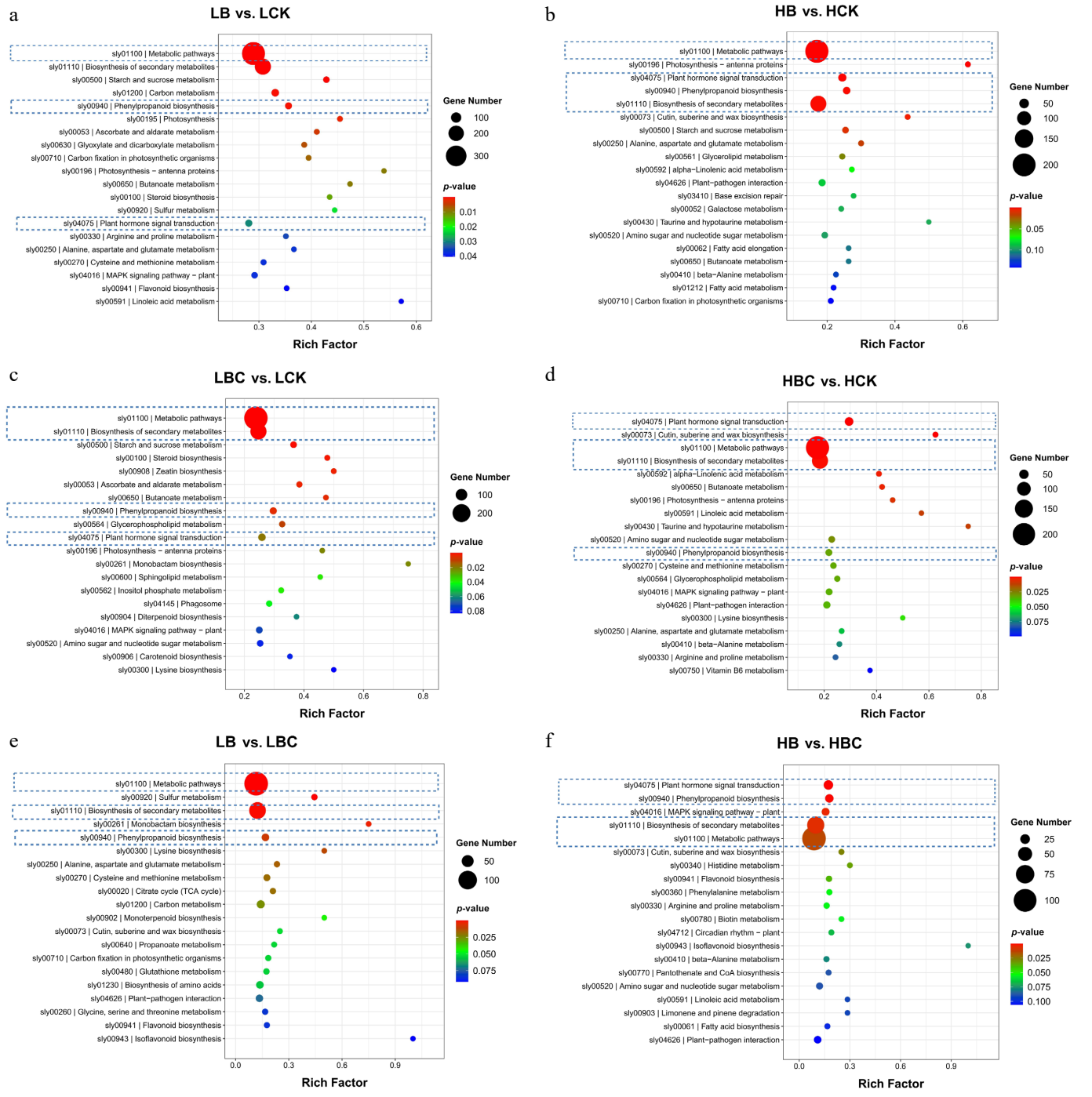

Fig. 5 KEGG enrichment analysis of DEGs between sample replicates within each tissue of tomato fruit. (a) LB vs. LCK, (b) HB vs. HCK, (c) LBC vs. LCK, (d) HBC vs. HCK, (e) LB vs. LBC, (f) HB vs. HBC.

Collectively, these findings indicate that silencing *POD* enhances susceptibility to ToBRFV infection in tomato, whereas silencing *CAD*, *C4H*, or *PAL*, confers increased resistance, thereby suppressing viral accumulation.

To further investigate the mechanisms underlying the observed differences in resistance, we assessed the accumulation of H_2O_2 and $O_2^{\bullet-}$ in *TRV-POD* plants and *TRV2-GFP* controls, both prior to, and following ToBRFV infection, using histochemical staining and quantitative assays. The results revealed significant alterations in ROS levels in the *TRV-POD* group compared to the *TRV2-GFP* control (Fig. 9). Notably, H_2O_2 levels were consistently higher in the *TRV-POD* group than in the *TRV2-GFP* controls, both pre- and post-infection (Fig. 9a, c). This increased accumulation of H_2O_2 exhibited a positive correlation with the pathogenic phenotypes observed, suggesting that POD plays a critical role in regulating ROS balance and enhancing plant defense mechanisms. Furthermore, the levels of $O_2^{\bullet-}$ were also significantly higher in the TRV-POD group before and after infection (Fig. 9b, d), indicating a marked increase in superoxide anion accumulation in these plants. These findings further support the notion that ROS plays a crucial role in the response to ToBRFV infection.

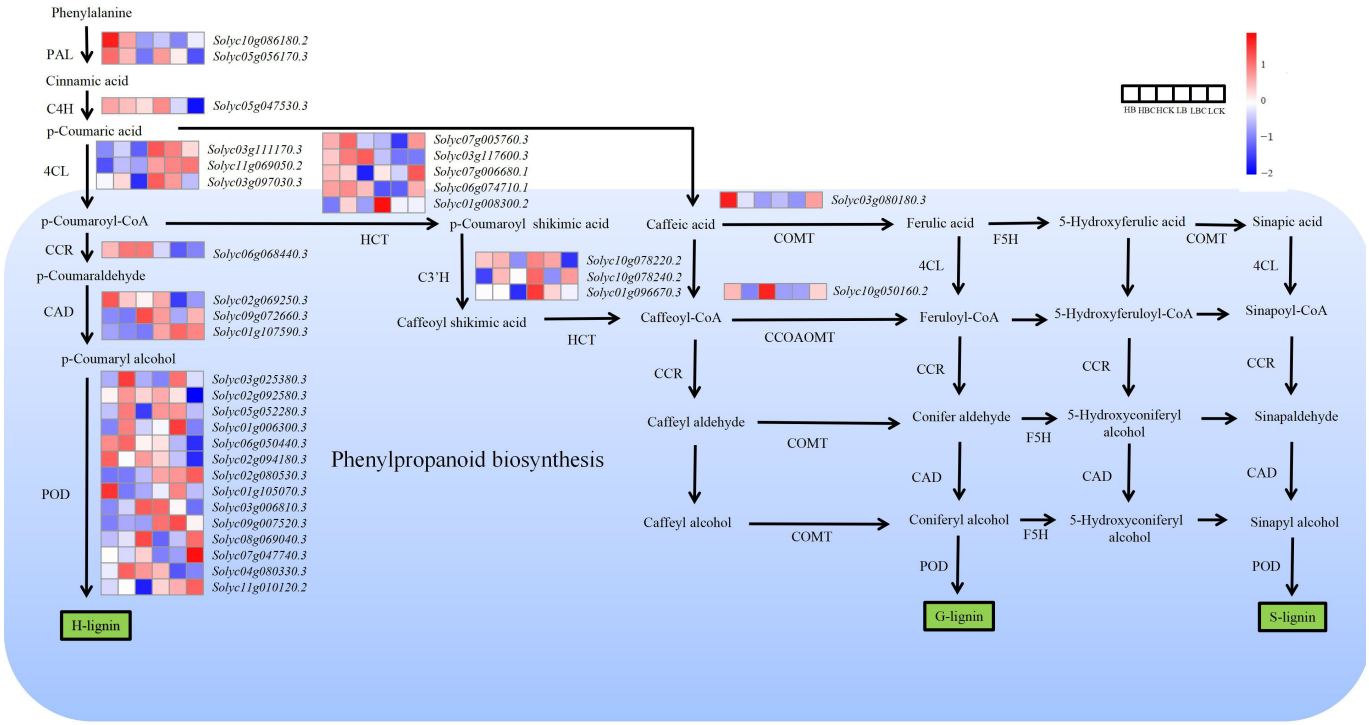

Fig. 6 Schematic illustration depicting the pathway analysis of DEGs associated with phenylalanine metabolism between sample replicates within each tissue of tomato fruit. The heatmap shows $\log_2$(FC), with red indicating higher expression and blue indicating lower expression, as indicated in the scale bar on the right. PAL, phenylalanine ammonialyase; C4H, cinnamate 4-hydroxylase; 4CL, 4-coumaroyl CoA ligase; CCR, cinnamoyl-CoA reductase; HCT, shikimate O-hydroxycinnamoyltransferase; CAD, cinnamyl-alcohol dehydrogenase; CCoAOMT, caffeoyl-CoAO-methyltransferase; C3H, 5-O-(4-coumaroyl)-d-quinate3-monooxygenase; POD, peroxidase; COMT, caffeicacid3-O-methyltransferase.

Overall, these findings underscore the importance of ROS regulation in the context of ToBRFV resistance, highlighting the pivotal role of POD in the management of reactive oxygen species and the resultant resistance of tomato plants to ToBRFV infection.

Discussion

ToBRFV has emerged as a significant threat to global tomato production, causing substantial losses in both yield and fruit quality[4,6–9]. The formation of localized brown, hardened lesions on tomato fruit induced by ToBRFV infection directly impairs their commercial value, representing a critical bottleneck for tomato quality improvement and disease-resistant breeding. However, the molecular regulatory mechanisms underlying this phenotypic alteration remain poorly understood. In this study, RNA-seq analysis combined with VIGS technology was used to systematically investigate the role of phenylpropanoid biosynthesis pathway genes in ToBRFV-infected tomato fruit. Our finding reveals the dual regulatory effects of these genes on fruit lesion formation and plant resistance, thereby providing valuable theoretical support for the genetic improvement of tomato disease resistance and quality.

Through RNA-seq analysis of fruit tissues at different developmental stages (HB, HBC, HCK, LB, LBC, and LCK) (Fig. 1), we identified 5,345 DEGs in the HB vs HCK comparison, and 4,926 DEGs in the HBC vs HCK comparison at the red fruit stage (Fig. 3a–c). At the green fruit stage, we detected 3,636 DEGs between LB and LCK, and 3,895 DEGs between LBC and LCK (Fig. 3d–f). Notably, the number of DEGs at the red-ripe stage was higher than that at the green-ripe stage, suggesting that tomato fruit may undergo a more sensitive or complex regulatory response to ToBRFV infection during this later developmental stage. This finding aligns with previous studies indicating that host defense responses can vary significantly with developmental stages due to factors such as hormonal changes, accumulation of secondary metabolites, and differences in gene expression patterns.

GO and KEGG enrichment analyses showed that DEGs across all comparison groups were significantly enriched in pathways related to phenylpropanoid biosynthesis, flavonoid biosynthesis, and plant hormone signal transduction. Among them, the phenylpropanoid biosynthesis pathway, a core secondary metabolic pathway in plants, plays a crucial role in regulating plant growth and development, and resisting biotic and abiotic stresses[18–22,40–42]. Lignin, a polymer derived from phenylpropanoids, is a key structural component of the plant cell wall and significantly contributes to resistance against pathogen invasion[21–24,26,27,43–48]. In this study, 34 DEGs associated with phenylpropanoid biosynthesis were identified in different tissues of ToBRFV-infected tomato fruit, and these genes exhibit highly diverse expression patterns across different fruit tissues and developmental stages. For example, genes encoding PAL enzymes, *Solyc05g056170.3* gene, had the higher expression levels in the infected group (B, BC), while *Solyc10g086180.2* exhibited higher expression in infected fruit at the red fruit stage, but downregulated expression in infected fruit at the green stage (Fig. 6). This differential expression pattern suggests that these genes may play distinct roles in ToBRFV infection-induced fruit lesion formation. Notably, genes encoding *PAL* (*Solyc05g056170.3*), *C4H* (*Solyc05g047530.3*), *CAD* (*Solyc02g069250.3*), and *POD* (*Solyc02g094180.3*) exhibited substantially higher expression levels in infected tissues than in healthy controls (Fig. 6). These four genes have been reported to participate in plant lignin synthesis. Thus, the phenylpropanoid pathway, known for its role in structural

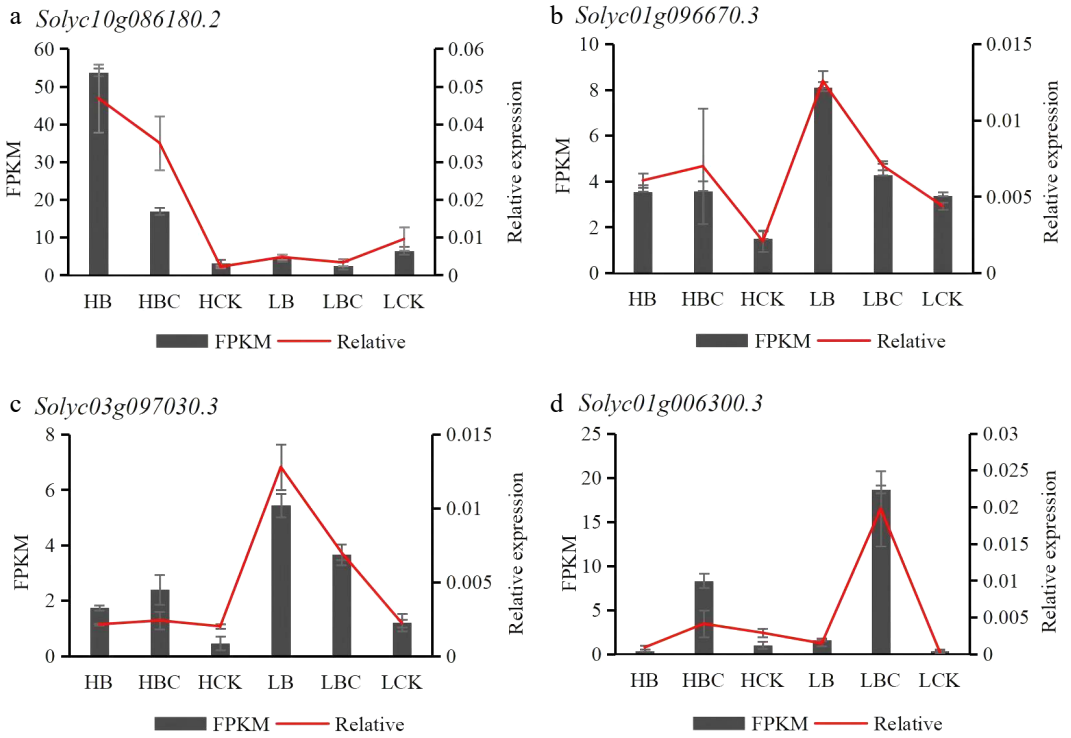

Fig. 7 RNA-seq results illustrating gene expression levels based on FPKM values and qRT-PCR measurements for the four selected DEGs. The red line chart displays the variations in qRT-PCR results across the groups, while the black bar chart depicts differences in RNA-seq data represented by FPKM values.

reinforcement and defense responses, is actively engaged during ToBRFV infection. Indeed, the accumulation of lignin, a primary product of this pathway, serves as a crucial factor in plant resistance against pathogens[26,27,49–52]. Our findings are consistent with previous studies highlighting the significant impact of lignin content on plant immunity and stress tolerance. For example, in *Arabidopsis*, the lignin content of *PAL* and *CAD* gene mutants was reduced by 20%–25% and 50%, respectively, compared with the wild type[48,49]. Ji et al.[50] reported that PpWRKY70 activated the expression of *PpPAL1*, leading to lignin accumulation in peach fruit. PpMYB306 was shown to repress *PpC4H* expression, accompanied by decreased lignin content[51]. Li et al.[22] demonstrated that during *Monilinia fructicola* infection, the expression levels of *PAL1* and *C4H* were upregulated in peach fruit, which was associated with lignin accumulation. In comparison to the AC tomato cultivar, the SH cultivar demonstrates elevated expression levels of genes associated with HCT, CAD, and POD enzymes, which may enhance the thickness of the secondary cell wall in SH leaves and facilitate the accumulation of H-lignin[12]. Additionally, T-DNA insertion mutants of *Arabidopsis* for *AtPOD2* and *AtPOD25* exhibited lower lignin content, with double mutations in these genes, further aggravating this phenotype[52]. In asparagus, *CCR*, *POD*, and *CCoAOMT* are critical genes involved in lignin biosynthesis, and their expression levels were significantly downregulated under shading conditions, resulting in decreased lignin content[53]. Collectively, these results indicate that *PAL* (*Solyc05g056170.3*), *C4H* (*Solyc05g047530.3*), *CAD* (*Solyc02g069250.3*), and *POD* (*Solyc02g094180.3*) are actively involved in the lignin biosynthesis process in response to ToBRFV infection, highlighting their significance in plant defense.

To further elucidate the biological roles of these key genes, VIGS technology was used to silence *PAL* (*Solyc05g056170.3*), *C4H* (*Solyc05g047530.3*), *CAD* (*Solyc02g069250.3*), and *POD* (*Solyc02g094180.3*) in tomato plants. Silencing of these four genes resulted in a significant reduction in lignin content, confirming their critical roles in lignin biosynthesis. These observations are consistent with findings in other species: for example, CsPOD25 in *Citrus sinensis* can maintain reactive oxygen species (ROS) homeostasis and regulate cell wall lignification, thereby conferring resistance to infection by *Xanthomonas citri* subsp. *citri* (Xcc)[54,55]; *Arabidopsis* T-DNA insertion mutants of *AtPOD2* and *AtPOD25* exacerbated reduced lignin content and structural changes in the stem[52]; in inbred maize lines, the expressions of the *CAD* gene related to lignin biosynthesis and lignin content in leaves were significantly positively correlated with drought tolerance[56]. Subsequently, these gene-silenced plants were mechanically inoculated with ToBRFV, and infection symptoms were observed. At 7 dpi, all groups exhibited mild symptoms, such as slight downward leaf curling. By 14 dpi, phenotypic observations showed that leaves in the *TRV-POD* group had more severe curling, while the *TRV-CAD*, *TRV-C4H*, and *TRV-PAL* groups displayed milder symptoms (Fig. 8d). Consistently, molecular detection revealed that the viral load of ToBRFV in the *TRV-POD* group was significantly higher than that in the *TRV2-GFP* control group, while the viral loads in the *TRV-CAD*, *TRV-C4H*, and *TRV-PAL* groups were significantly lower than those in the control group (Fig. 8e). Previous studies have established that ROS serve dual roles in plants, functioning both as signaling molecules in defense pathways, and as damaging agents under stress conditions[57,58]. In our study, *TRV-POD* plants exhibited markedly enhanced ROS accumulation, further improving our understanding of the interplay between oxidative stress and disease resistance. Specifically, elevated levels of hydrogen peroxide (H_2O_2) and superoxide anions ($O_2^{\bullet-}$) in the *TRV-POD* group were positively correlated with the severity of pathogenic phenotypes, indicating a critical role of POD in regulating oxidative stress and mediating defensive responses against ToBRFV.

Collectively, our findings indicate that silencing the *POD* (*Solyc02g094180.3*) gene reduced lignin content and increased tomato susceptibility to ToBRFV infection, suggesting a correlation between elevated lignin levels and the formation of brown necrotic spots in

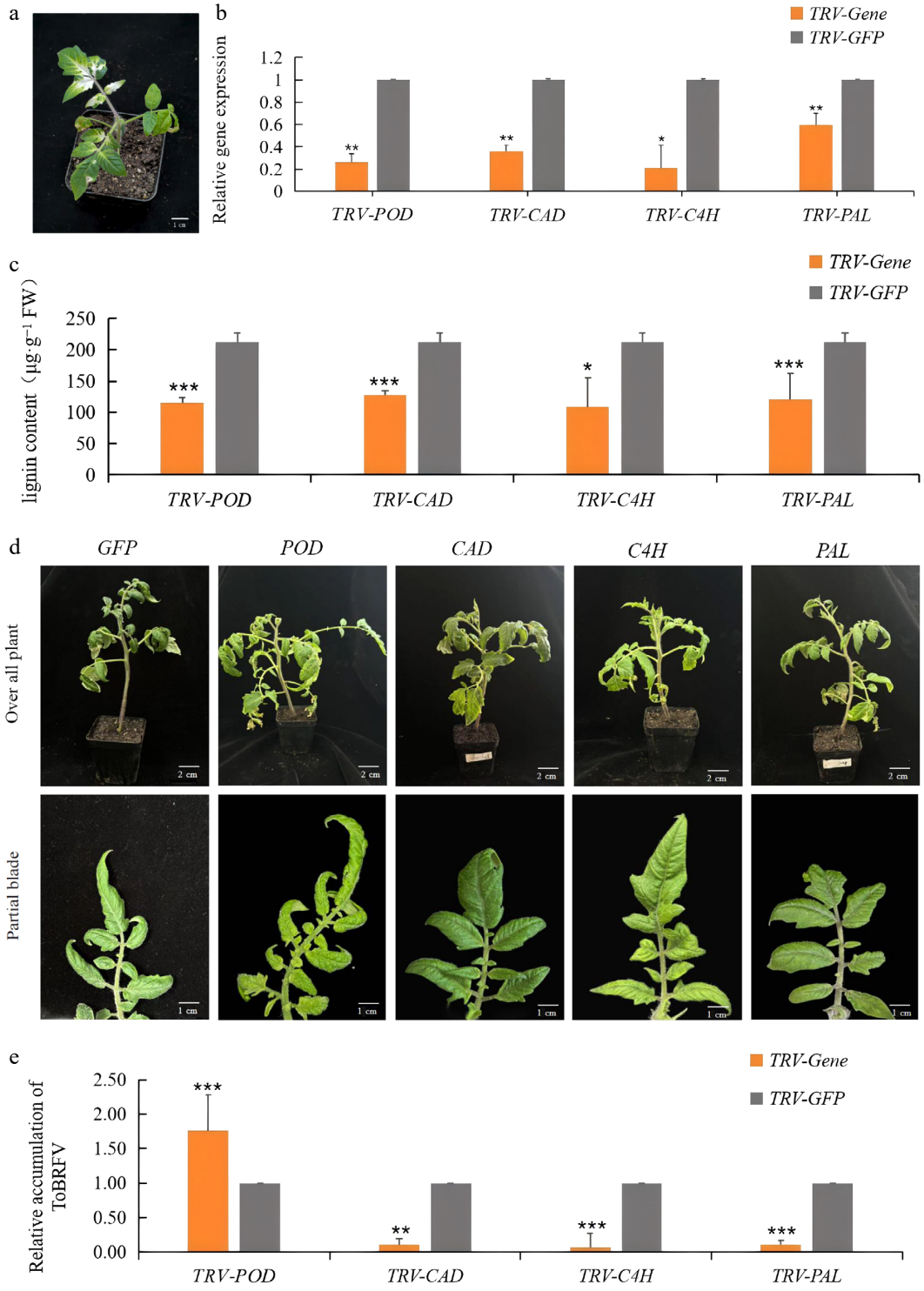

Fig. 8 Infection status of ToBRFV following downregulation of candidate genes. (a) Symptoms of plants after silencing of *PDS* gene. (b) Expression of candidate genes in CK and gene silenced plants. (c) Lignin content in CK and different gene-silenced plants. (d) Changes in phenotypes of CK and silenced plants after inoculation with ToBRFV for 14 d. (e) RT-qPCR analysis of ToBRFV genomic RNA in CK and gene-silenced plants at 14 dpi. Each value indicates the mean ± standard deviation of three biological replicates. *, **, and *** indicate significant differences between CK and silenced plants with $p < 0.05$, $p < 0.01$, $p < 0.001$, respectively, as determined by *t*-test.

ToBRFV-infected fruit. Although lignin accumulation can strengthen structural barriers against pathogens, it may concurrently compromise fruit quality by inducing undesirable traits such as increased hardness and abnormal coloration. Therefore, it is crucial to carefully navigate the 'defense-quality' trade-off when developing breeding strategies for improving tomato resistance to ToBRFV.

Conclusions

In conclusion, this study systematically explored the regulatory role of key genes in the phenylpropanoid biosynthesis pathway during ToBRFV infection of tomato fruit through transcriptome sequencing and VIGS technology. The results confirmed that the

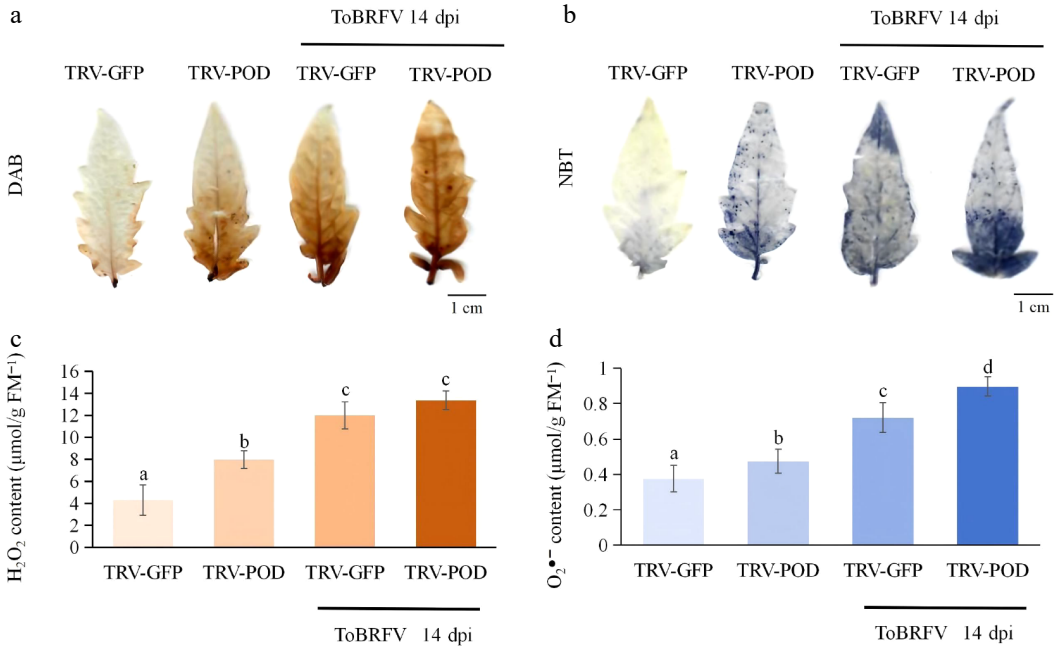

Fig. 9 ROS accumulation in *TRV-POD* tomato plants pre- and post-ToBRFV infection (14 dpi). (a) Visualization of H_2O_2 via diaminobenzidine (DAB) staining. (b) Visualization of $O_2^{\bullet-}$ via nitroblue tetrazolium (NBT) staining. (c) Quantification of H_2O_2 content. (d) Quantification of $O_2^{\bullet-}$ content. Data is presented as mean ± standard deviation (n = 3 biological replicates), and significant differences were determined by one-way ANOVA followed by multiple comparison tests.

phenylpropanoid biosynthesis pathway is closely involved in tomato response to ToBRFV infection, and four key genes, *PAL* (*Solyc05g056170.3*), *C4H* (*Solyc05g047530.3*), *CAD* (*Solyc02g069250.3*), and *POD* (*Solyc02g094180.3*), play distinct regulatory roles in this process. Specifically, POD enhances tomato resistance to ToBRFV by maintaining ROS homeostasis and promoting lignin synthesis, while *PAL*, *C4H*, and *CAD* negatively regulate resistance, and their high expression contributes to the formation of brown and hardened lesions on fruit by promoting excessive lignin deposition. These findings not only clarify the molecular mechanism underlying the formation of ToBRFV-induced tomato fruit lesions from the perspective of secondary metabolism, but also fill the gap in the study of genetic regulation of ToBRFV-induced fruit quality deterioration. More importantly, the key genes identified in this study provide valuable target genes for the genetic improvement of tomato, laying a theoretical foundation for breeding new tomato varieties with both high resistance to ToBRFV, and excellent fruit quality. Future research focusing on the upstream regulatory network of these key genes and their interaction mechanisms with other metabolic pathways will further deepen the understanding of tomato-ToBRFV interaction, and provide more effective strategies for the sustainable development of the global tomato industry.

Author contributions

The authors confirm their contributions to the paper as follows: conceptualization, methodology: Cao X, Yang K, Ren J, Wu Z; data curation: Cao X, Yu Y, Zheng T, Fu S, Li A; investigation: Cao X, Yu Y, Zheng T; writing – original draft preparation: Cao X, Wang Z; formal analysis: Cao X, Yang K, Ren J; supervision: Yang K, Ren J, Wu Z; resources: Yang K, Ren J; writing – review and editing: Cao X, Ren J, Wu Z; project administration, funding acquisition: Ren J. All authors reviewed the results and approved the final version of the manuscript.

Data availability

All data generated or analyzed during this study are included in this published article and its supplementary information files.

Acknowledgments

We gratefully acknowledge the support and contributions from all participants and institutions involved in this research. We are especially grateful to Mr. Yuhao Han for providing the original isolate of ToBRFV and the key tomato samples, which were pivotal to the study. The research was supported by National Natural Science Foundation of China (32202282).

Conflict of interest

The authors declare that they have no conflict of interest.

Supplementary information accompanies this paper online at: https://doi.org/10.48130/vegres-0026-0006.

Dates

Received 31 October 2025; Revised 13 January 2026; Accepted 9 February 2026; Published online 11 May 2026

References

[1] Zhang J, Ren J, Yang J, Fu S, Zhang X, et al. 2023. Evaluation of SNP fingerprinting for variety identification of tomato by DUS testing. *Agriculture Communications* 1:100006

[2] Zhang J, Lyu H, Chen J, Cao X, Du R, et al. 2024. Releasing a sugar brake generates sweeter tomato without yield penalty. *Nature* 635:647–656

[3] Ali MY, Sina AAI, Khandker SS, Neesa L, Tanvir EM, et al. 2020. Nutritional composition and bioactive compounds in tomatoes and their impact on human health and disease: a review. *Foods* 10:45

[4] Ma HY, Kong Y, Geng C, Tian YP, Jiang J, et al. 2025. RabE1a- and SEC10b-mediated exocytosis and AP2β-mediated endocytosis are involved in the intracellular transport of tobamoviruses. *Plant Biotechnology Journal* 23:3237–3253

[5] Luria N, Smith E, Reingold V, Bekelman I, Lapidot M, et al. 2017. A new Israeli *tobamovirus* isolate infects tomato plants harboring *Tm-2*^{2} resistance genes. *PLoS One* 12:e0170429

[6] Ishikawa M, Yoshida T, Matsuyama M, Kouzai Y, Kano A, et al. 2022. Tomato brown rugose fruit virus resistance generated by quadruple knockout of homologs of *TOBAMOVIRUS MULTIPLICATION1* in tomato. *Plant Physiology* 189:679–686

[7] Zhou J, Gilliard A, Ling KS. 2024. Tomato brown rugose fruit virus is transmissible through a greenhouse hydroponic system but may be inactivated by cold plasma ozone treatment. *Horticulturae* 10:416

[8] Zhang S, Griffiths JS, Marchand G, Bernards MA, Wang A. 2022. *Tomato brown rugose fruit virus*: An emerging and rapidly spreading plant RNA virus that threatens tomato production worldwide. *Molecular Plant Pathology* 23:1262–1277

[9] Salem NM, Jewehan A, Aranda MA, Fox A. 2023. Tomato brown rugose fruit virus pandemic. *Annual Review of Phytopathology* 61:137–164

[10] Yan ZY, Zhao MS, Ma HY, Liu LZ, Yang GL, et al. 2021. Biological and molecular characterization of tomato brown rugose fruit virus and development of quadruplex RT-PCR detection. *Journal of Integrative Agriculture* 20:1871–1879

[11] Chen C, Huang T, Wang LX, Xiong JS, Li MY, et al. 2025. High-throughput transcriptomic analysis of circadian rhythm of flavonoid metabolism under different photoperiods in celery. *Vegetable Research* 5:e028

[12] Wang M, Wang Y, Li X, Zhang Y, Chen X, et al. 2024. Integration of metabolomics and transcriptomics reveals the regulation mechanism of the phenylpropanoid biosynthesis pathway in insect resistance traits in *Solanum habrochaites*. *Horticulture Research* 11:uhad277

[13] Ren J, Fu S, Wang H, Wang W, Wang X, et al. 2024. Comparative transcriptome analysis of cucumber fruit tissues reveals novel regulatory genes in ascorbic acid biosynthesis. *PeerJ* 12:e18327

[14] Li C, Zhang Q, Wang X, Liu Z, Zhang X, et al. 2025. Transcriptomic and metabolomic analyses reveal molecular mechanisms of tobacco mosaic virus (TMV) resistance in *Nicotiana tabacum* L. *BMC Plant Biology* 25:1029

[15] Maleki N, Ghorbani A, Rostami M, Maina S. 2025. Elucidating long non-coding RNA networks in tomato plants in response to *Funneliformis mosseae* colonization and cucumber mosaic virus infection. *BMC Plant Biology* 25:495

[16] Liu M, Kang B, Wu H, Aranda MA, Peng B, et al. 2023. Transcriptomic and metabolic profiling of watermelon uncovers the role of salicylic acid and flavonoids in the resistance to cucumber green mottle mosaic virus. *Journal of Experimental Botany* 74:5218–5235

[17] Romero-Rodríguez B, Petek M, Jiao C, Križnik M, Zagorščak M, et al. 2023. Transcriptional and epigenetic changes during tomato yellow leaf curl virus infection in tomato. *BMC Plant Biology* 23:651

[18] Kalapos B, Juhász C, Balogh E, Kocsy G, Tóbiás I, et al. 2021. Transcriptome profiling of pepper leaves by RNA-Seq during an incompatible and a compatible pepper-tobamovirus interaction. *Scientific Reports* 11:20680

[19] Naoumkina MA, Zhao Q, Gallego-Giraldo L, Dai X, Zhao PX, et al. 2010. Genome-wide analysis of phenylpropanoid defence pathways. *Molecular Plant Pathology* 11:829–846

[20] Zhang CH, Ma T, Luo WC, Xu JM, Liu JQ, et al. 2015. Identification of *4CL* genes in desert poplars and their changes in expression in response to salt stress. *Genes* 6:901–917

[21] Li Q, Liu Z, Jiang Z, Jia M, Hou Z, et al. 2025. Phenylalanine metabolism-dependent lignification confers rhizobacterium-induced plant resistance. *Plant Physiology* 197:kiaf016

[22] Li Q, Chen Y, Wei Y, Jiang S, Ye J, et al. 2025. PpMYC2 and PpJAM2/3 antagonistically regulate lignin synthesis to cope with the disease in peach fruit. *Plant Biotechnology Journal* 23:3524–3539

[23] Liu Q, Luo L, Zheng L. 2018. Lignins: biosynthesis and biological functions in plants. *International Journal of Molecular Sciences* 19:335

[24] Boerjan W, Ralph J, Baucher M. 2003. Lignin biosynthesis. *Annual Review of Plant Biology* 54:519–546

[25] Lavhale SG, Kalunke RM, Giri AP. 2018. Structural, functional and evolutionary diversity of 4-coumarate-CoA ligase in plants. *Planta* 248:1063–1078

[26] Sun H, Li H, Huang M, Gao Z. 2024. Expression and function analysis of phenylalanine ammonia-lyase genes involved in Bamboo lignin biosynthesis. *Physiologia Plantarum* 176:e14444

[27] Wang H, Li Y, Wang X, Liu S, Fan F, et al. 2025. Cyclo (Pro-Tyr) upregulates *GmPOD53L* to enhance soybean resistance to cyst nematode (*Heterodera glycines* Ichinohe). *Frontiers in Plant Science* 16:1628555

[28] Li X, Huang X, Wen M, Yin W, Chen Y, et al. 2023. Cytological observation and RNA-seq analysis reveal novel miRNAs high expression associated with the pollen fertility of neo-tetraploid rice. *BMC Plant Biology* 23:434

[29] Martin M. 2011. Cutadapt removes adapter sequences from high-throughput sequencing reads. *EMBnet Journal* 17:10–12

[30] Thompson O, von Meyenn F, Hewitt Z, Alexander J, Wood A, et al. 2020. Low rates of mutation in clinical grade human pluripotent stem cells under different culture conditions. *Nature Communications* 11:1528

[31] Kim D, Langmead B, Salzberg SL. 2015. HISAT: a fast spliced aligner with low memory requirements. *Nature Methods* 12:357–360

[32] Pertea M, Pertea GM, Antonescu CM, Chang TC, Mendell JT, et al. 2015. StringTie enables improved reconstruction of a transcriptome from RNA-seq reads. *Nature Biotechnology* 33:290–295

[33] Lê S, Josse J, Husson F. 2008. FactoMineR: an R Package for multivariate analysis. *Journal of Statistical Software* 25:1–18

[34] Love MI, Huber W, Anders S. 2014. Moderated estimation of fold change and dispersion for RNA-seq data with DESeq2. *Genome Biology* 15:550

[35] Livak KJ, Schmittgen TD. 2001. Analysis of relative gene expression data using real-time quantitative PCR and the $2^{-\Delta\Delta CT}$ method. *Methods* 25:402–408

[36] Jiang L, Ling J, Zhao J, Yang Y, Yang Y, et al. 2023. Chromosome-scale genome assembly-assisted identification of *Mi-9* gene in *Solanum arcanum* accession LA2157, conferring heat-stable resistance to *Meloidogyne incognita*. *Plant Biotechnology Journal* 21:1496–1509

[37] Gatzek S, Wheeler GL, Smirnoff N. 2002. Antisense suppression of l-galactose dehydrogenase in *Arabidopsis thaliana* provides evidence for its role in ascorbate synthesis and reveals light modulated l-galactose synthesis. *The Plant Journal* 30:541–553

[38] Thordal-Christensen H, Zhang Z, Wei Y, Collinge DB. 1997. Subcellular localization of H_2O_2 in plants. H_2O_2 accumulation in papillae and hypersensitive response during the barley—powdery mildew interaction. *The Plant Journal* 11:1187–1194

[39] Karpinska B, Foyer CH. 2024. Superoxide signalling and antioxidant processing in the plant nucleus. *Journal of Experimental Botany* 75:4599–4610

[40] Wu Z, Singh SK, Lyu R, Pattanaik S, Wang Y, et al. 2022. Metabolic engineering to enhance the accumulation of bioactive flavonoids licochalcone A and echinatin in *Glycyrrhiza inflata* (Licorice) hairy roots. *Frontiers in Plant Science* 13:932594

[41] Dong NQ, Lin HX. 2021. Contribution of phenylpropanoid metabolism to plant development and plant–environment interactions. *Journal of Integrative Plant Biology* 63:180–209

[42] Gesteiro N, Butrón A, Estévez S, Santiago R. 2021. Unraveling the role of maize (*Zea mays* L.) cell-wall phenylpropanoids in stem-borer resistance. *Phytochemistry* 185:112683

[43] Jan R, Khan M, Asaf S, Lubna, Asif S, et al. 2022. Bioactivity and therapeutic potential of kaempferol and quercetin: new insights for plant and human health. *Plants* 11:2623

[44] Ma QH, Zhu HH, Qiao MY. 2018. Contribution of both lignin content and sinapyl monomer to disease resistance in tobacco. *Plant Pathology* 67:642–650

[45] Karmanov A, Kocheva L, Belyy V, Kanarsky A, Semenov E, et al. 2023. Structural features and antioxidant behavior of lignin polymers

isolated from various woody plants. *Biocatalysis and Agricultural Biotechnology* 54:102969

[46] Zhao Q. 2016. Lignification: flexibility, biosynthesis and regulation. *Trends in Plant Science* 21:713−721

[47] Bonawitz ND, Chapple C. 2010. The genetics of lignin biosynthesis: connecting genotype to phenotype. *Annual Review of Genetics* 44:337−363

[48] Huang J, Gu M, Lai Z, Fan B, Shi K, et al. 2010. Functional analysis of the Arabidopsis *PAL* gene family in plant growth, development, and response to environmental stress. *Plant Physiology* 153:1526−1538

[49] Thévenin J, Pollet B, Letarnec B, Saulnier L, Gissot L, et al. 2011. The simultaneous repression of CCR and CAD, two enzymes of the lignin biosynthetic pathway, results in sterility and dwarfism in *Arabidopsis thaliana*. *Molecular Plant* 4:70−82

[50] Ji N, Wang J, Li Y, Li M, Jin P, et al. 2021. Involvement of *PpWRKY70* in the methyl jasmonate primed disease resistance against *Rhizopus stolonifer* of peaches via activating phenylpropanoid pathway. *Postharvest Biology and Technology* 174:111466

[51] Li Y, Ji N, Zuo X, Zhang J, Zou Y, et al. 2023. Involvement of PpMYB306 in Pichia guilliermondii-induced peach fruit resistance against Rhizopus stolonifer. *Biological Control* 177:105130

[52] Shigeto J, Itoh Y, Hirao S, Ohira K, Fujita K, et al. 2015. Simultaneously disrupting *AtPrx2*, *AtPrx25* and *AtPrx71* alters lignin content and structure in *Arabidopsis* stem. *Journal of Integrative Plant Biology* 57:349−356

[53] Ma J, Li X, He M, Li Y, Lu W, et al. 2023. A joint transcriptomic and metabolomic analysis reveals the regulation of shading on lignin biosynthesis in asparagus. *International Journal of Molecular Sciences* 24:1539

[54] Li Q, Qin X, Qi J, Dou W, Dunand C, et al. 2020. CsPrx25, a class III peroxidase in *Citrus sinensis*, confers resistance to citrus bacterial canker through the maintenance of ROS homeostasis and cell wall lignification. *Horticulture Research* 7:192

[55] Fu J, Fan J, Zhang C, Fu Y, Xian B, et al. 2024. High-throughput screening system of citrus bacterial canker-associated transcription factors and its application to the regulation of citrus canker resistance. *Journal of Integrative Agriculture* 23:155−165

[56] Hu Y, Li WC, Xu YQ, Li GJ, Liao Y, et al. 2009. Differential expression of candidate genes for lignin biosynthesis under drought stress in maize leaves. *Journal of Applied Genetics* 50:213−223

[57] Li Q, Ai G, Shen D, Zou F, Wang J, et al. 2019. A *Phytophthora capsici* effector targets ACD11 binding partners that regulate ROS-mediated defense response in *Arabidopsis*. *Molecular Plant* 12:565−581

[58] Bi G, Hu M, Fu L, Zhang X, Zuo J, et al. 2022. The cytosolic thiol peroxidase PRXIIB is an intracellular sensor for H_2O_2 that regulates plant immunity through a redox relay. *Nature Plants* 8:1160−1175